THE UNIVERSITY OF ROCHESTER

THE INSTITUTE OF OPTICS

ROCHESTER, NEW YORK

TECHNICAL NOTE #8

Structure in the Optical Absorption Edge of Amorphous Selenium

Dean Brinton McKenney

Institute of Optics
University of Rochester
Rochester, New York

NASw-107
Responsible Investigator
R. E. Hopkins

August, 1965

STRUCTURE IN THE OPTICAL ABSORPTION EDGE OF AMORPHOUS SELENIUM

by

Dean Brinton McKenney

Submitted in Partial Fulfillment

of the

Requirements for the Degree

MASTER OF SCIENCE

Supervised by Professors Kenneth J. Teegarden and Robert M. Blakney

Institute of Optics

The University of Rochester

Rochester, New York

1965

VITA

The author was born in Newton, Massachusetts, on March 1, 1940. He did his undergraduate work at Bowdoin College where he received the Bachelor of Arts degree with honors in Physics in June, 1962.

In September, 1962, the author started graduate study in the Institute of Optics at the University of Rochester, completing his study for the Master of Science degree in 1965. During this period he has studied the optical properties of solids under the direction of Professors Kenneth J. Teegarden and Robert M. Blakney. During the academic year 1962-1963 he held the New England Section of the Optical Society of America scholarship, and the Walter S. Baird fellowship from 1962-1964. He has also held research assistantships during the 1963-1965 period.

ACKNOWLEDGEMENTS

The author would like to express his appreciation to Professors Kenneth J. Teegarden and Robert M. Blakney for their guidance, inspriation and support during the course of this investigation. It is a pleasure to also extend thanks to Professor Robert S. Knox for many helpful discussions with regard to the theoretical aspects of this investigation.

It is also a pleasure to acknowledge the helpful suggestions in discussions with Barry Bebb and Hubert Grunwald who both contributed to the ideas of this investigation.

The author is also indebted to John O'Brien for his advice in the experimental aspects of this work. Special thanks are given to Mr. Robert Horner for the design of several pieces of the experimental apparatus, and to Mr. Rudolph Hamberger for his care in building much of this equipment.

A debt of gratitude is owed to The National Aeronautics and Space Administration for financial support of this research under Contract Number NASw-107.

ABSTRACT

The absorption spectrum near the band edge of amorphous selenium was measured at temperatures between 295°K and 20°K on evaporated samples with and without substrates. A large difference between the two types of samples was noted especially at low temperatures. Structure in the absorption spectrum of unsupported samples similar to that observed in other semiconductors was analyzed and it is suggested that this structure is caused by indirect transitions between the valence band and the conduction band and by the formation of indirect excitons. The energy of the phonon assisting in the indirect transitions was found to be 0.023 eV. The binding energy of the exciton was 0.076 eV, and the energy of the indirect band gap was 1.717 eV at room temperature, increasing nearly with temperature by 7.4×10^{-4} eV/°K over a wide range of temperatures.

These results are compared with other experimental observations for both hexagonal and amorphous selenium and with recent energy band calculations. The results are explained in terms of a band model for amorphous selenium which has band minima on the hexagonal plane perpendicular to the direction of the c-axis in the first Brillouin zone of hexagonal selenium. The band scheme is justified by the existence of short range order which exists in small regions of the amorphous material.

Author

TABLE OF CONTENTS

LIST OF TABLES

LIST OF FIGURES

CHAPTER I

INTRODUCTION

In the past ten years experimental and theoretical advances in the study of the optical absorption spectra of semiconductors have contributed greatly to the understanding of these materials. The onset of strong optical absorption near the visible portion of the spectrum is known to be associated with the excitation of electrons from the valence band, across the forbidden gap, to the conduction band, or with the formation of excitons. In most semiconductors, the absorption coefficient rises several orders of magnitude in only a fraction of an electron volt. Location of this absorption edge then gives a rough measure of the band gap of the material. The electrical properties of semiconductors are influenced strongly by the electronic states just above and below the band gap. It is, in theory, possible to determine these states from optical measurements. Therefore, careful measurement and analysis of the optical absorption edge is an important element in the study of the properties of a semiconductor.

Although the edge has been located for many semiconductors, careful analysis of the edge has been made for only a few. Probably the best-known and most

extensive work has been carried out on germanium and silicon[1-4]. In these materials a detailed knowledge of the band structure has been gained from the optical absorption measurements, together with other experiments such as cyclotron resonance[5], galvano-magnetic effects, and magneto absorption to name a few[6]. The end result is that the energy band structures for these materials are now known to a high degree of precision and certainty.

All of the materials for which detailed measurement and analysis of the optical absorption edge have been made have been nearly perfect crystals, partly because a precise band structure with specific symmetry is defined only for such an orderly array of atoms. In this work, the optical absorption edge of amorphous selenium is examined. This material can be prepared either by rapid cooling from the molten phase or by vacuum evaporation. Laue x-ray diffraction patterns show no apparent order, but studies using other x-ray techniques show that considerable order exists over regions about 10Å in size[7]. The structure is similar to hexagonal selenium which consists of spiral chains having three atoms per turn. The equivalent atoms on adjacent chains form a hexagonal network. The nearest neighbor lies along the chain at a distance of 2.32Å and a bond angle of 105.5°, and the second nearest neighbors are located on adjacent chains

at a distance of 3.46Å. Figure 1 is a schematic diagram of the hexagonal structure[8,9]. The nearest neighbor distance in amorphous selenium is also 2.32Å, but the next nearest neighbor distance is increased to 3.80Å[7].

The purpose of this work was to measure and analyze the onset of absorption in amorphous selenium in a manner similar to that used for other crystalline semiconductors. Extensive optical measurements in the region of the absorption edge have been made previously[10-16], but have not been analyzed in such a manner. The existance of short-range order has prompted this author and others[17-23] to interpret measurements in terms of the band theory. The theory of the optical absorption edge has been derived elsewhere for several cases, and a review of this work is presented in Chapter II. In order to get meaningful results from the absorption measurements the functional dependance of the absorption coefficient on both photon energy and temperature must be known accurately. The experimental techniques used in obtaining this information in the region from 1.5 - 2.0 eV are presented in Chapter III together with some new techniques used to prepare the samples. The results of the measurements are presented in Chapter IV, where it is suggested that the low values of the absorption coefficient are caused by indirect transitions to the conduction band and the exciton band.

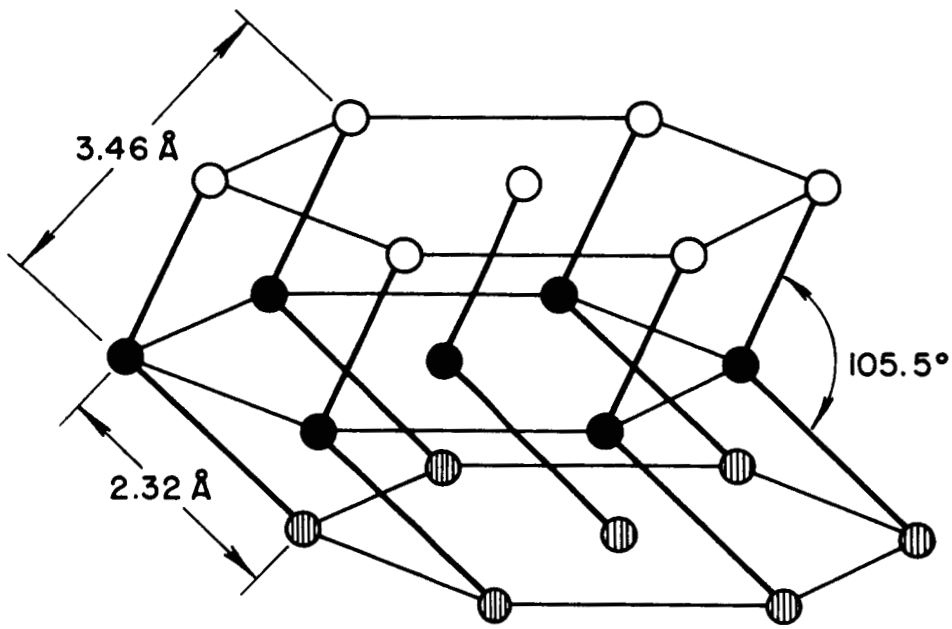

Fig. 1. The structure of hexagonal selenium

The indirect band gap at room temperature is found to be 1.717 $\pm$ 0.005 eV and the binding energy of the exciton is 0.076 $\pm$ 0.01 eV. The indirect band gap decreases with increasing temperature by 7.4×10^{-4} eV/°K, over a large temperature range. The absorption spectrum which yielded these results was measured from 20°K to 295°K on thin evaporated samples without substrates. The results are discussed in the light of recent band calculations in Chapter V. The most recent calculation would lead one to expect only direct transitions so that a minimum in the conduction band is proposed in a different symmetry direction. There are many different experiments that could be done which would further demonstrate the existence of an indirect band gap in amorphous selenium. Some of these are suggested in Chapter VI, as well as further measurements that could give a better understanding of this material.

CHAPTER II

THEORY OF THE OPTICAL ABSORPTION-EDGE SPECTRUM

1. Introduction

In this chapter the theory of the optical absorption spectrum is reviewed. We shall be interested in expressions for the absorption coefficient for the cases of direct and indirect transitions for single, non-degenerate bands. Only the results of the calculations are presented here, and the reader should refer to a review article by T. P. McLean[24] for a full discussion. The expressions which follow were taken from this article with only slight modifications in form and notation.

2. Definitions

The optical absorption coefficient is a property of the material and is defined as the energy removed per unit time and volume from a beam of unit intensity. Let $\vec{\mathcal{E}}$ be the electric field vector in a medium of refractive index n such that the energy density in the medium is $n\langle\vec{\mathcal{E}}\rangle^2/4\pi$. If $w(E)$ is the probability per unit time per unit volume that a photon of energy $E=\hbar\omega$ has been absorbed causing an electronic transition, then the absorption coefficient is given by

$$\alpha(E)=\frac{4\pi}{n\langle\vec{\mathcal{E}}\rangle^2}\,\frac{E}{c}\,w(E) \qquad (2\text{-}1)$$

where c is the velocity of light. The problem is to calculate the transition probability $w(E)$. This is done formally using the semi-classical theory of radiation.

The Hamiltonian for the system in its simplest form consists of two parts: the atomic Hamiltonian and the interaction or radiation Hamiltonian given by

$$H_R = -\frac{e}{mc}\sum_j \vec{A}(\vec{r}_j,t)\cdot\vec{p}_j \quad + \underline{O}(A^2) \qquad (2\text{-}2)$$

where $\vec{A}$ is the vector potential of the radiation field, and the summation runs over the valence electrons, or more precisely all of the electrons in the crystal. Terms are added to Eq. (2-2) to treat the more complex cases. The probability that a transition has occured in time t from the ground state $|0\rangle$ to a state $|\vec{k}_v,\vec{k}_c\rangle$ described by the wave vectors $\vec{k}_v$ and $\vec{k}_c$ in the valence and conduction bands respectively is given by

$$w(E)=\frac{2}{V}\frac{2\pi}{\hbar}\sum_{\vec{k}_v}\sum_{\vec{k}_c}|\langle\vec{k}_v,\vec{k}_c|H_R|0\rangle|^2\,\delta[E(\vec{k}_c)-E(k_v)-E]\,. \qquad (2\text{-}3)$$

The factor of 2 accounts for the spin states of the electron. In this equation V is the volume of the crystal, and $E(\vec{k}_i)$ is the energy associated with an electron in the band i with wave vector $\vec{k}_i$. The summation should extend over all possible states while the δ-function insures conservation of energy.

Thus, to predict the absorption coefficient, one must have accurate knowledge of the wave functions of the electrons and must also be able to perform the summation over all states. This is generally a task too formidable to be realistic and impossible in the case of amorphous selenium where the symmetry associated with a particular atom can only be approximated. It is possible to treat special cases with simplifying assumptions to get useful results as is shown in the next two sections.

3. Direct Transitions

The simplest case that can be treated is for the excitation between two parabolic bands whose extrema lie at the same point in $\vec{k}$ -space. If we assume that the electronic states may be represented by Bloch functions, and convert the summation in Eq. (2-3) to an integration in the usual way, the phase factors will yield a δ -function of the form $\delta(\vec{k}_v - \vec{k}_c - \vec{q})$ where $\vec{q}$ is the wave vector of the photon. Since the wave vector for photons of energy $\sim$ 2 eV is very small in comparison to the size of the electronic wave vectors, it is assumed in this case that only vertical or direct transitions can occur as shown by the heavy arrow in Fig. 2(a). In this case, the absorption coefficient is given by

$$\alpha(E) = \frac{\text{const.}}{E} \int dk \left| M_{\vec{k}_c \vec{k}_c} \right|^2 k^2 \, \delta\left[E_g - E + \frac{\hbar^2 k^2}{2\mu^*} \right] \qquad (2\text{-}4)$$

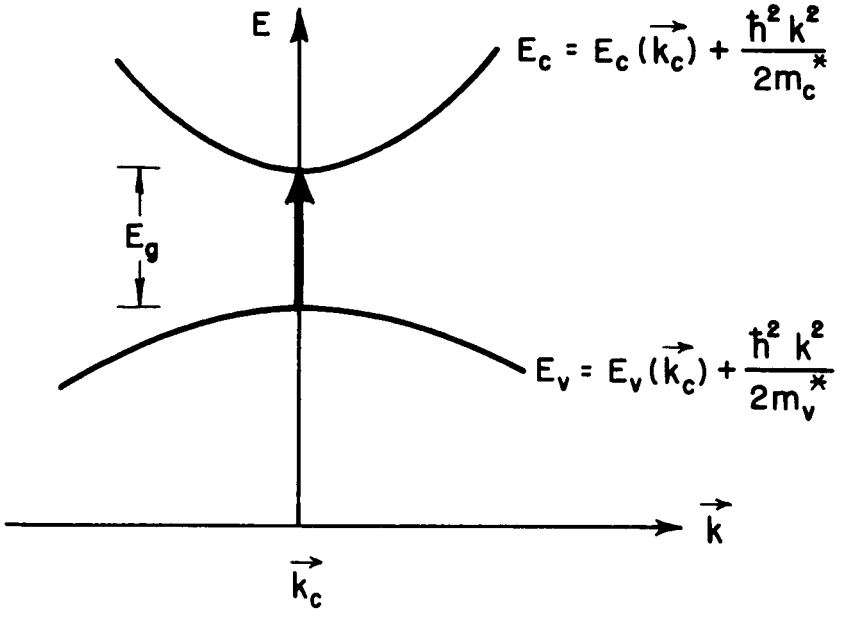

(a)

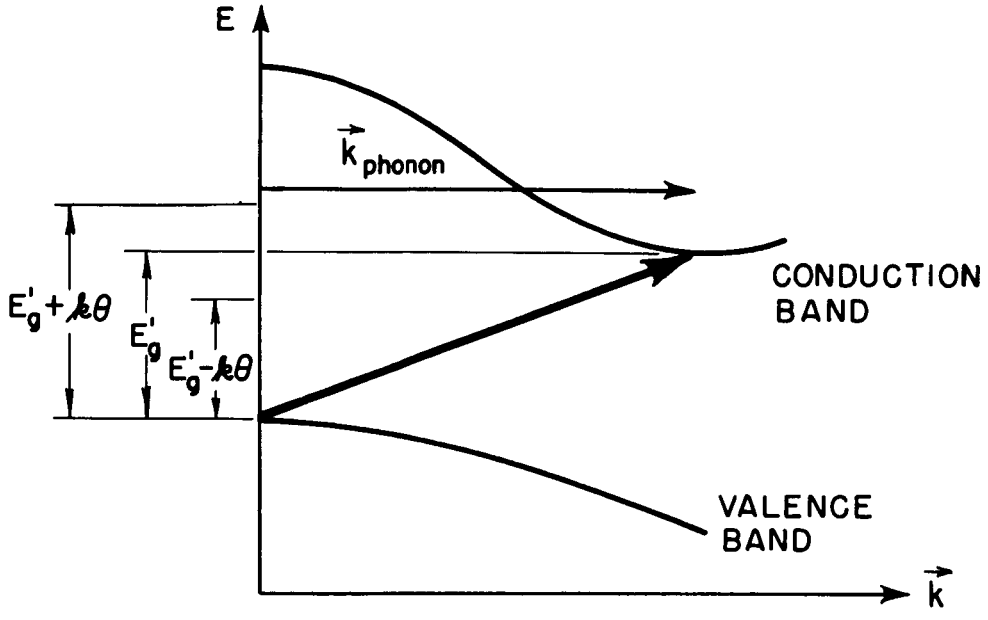

(b)

Fig. 2. Energy bands showing (a) direct and (b) indirect transitions

where

$$M_{k_v,k_c} = \int_{\substack{\text{unit}\\ \text{cell}}} d\vec{r}\; u^*_{\vec{k}_c}(\vec{r})\left(\vec{e}\cdot\vec{\nabla} + i\,\vec{e}\cdot\vec{k}_c\right) u_{\vec{k}_c}(\vec{r}) \qquad (2\text{-}5)$$

and μ^* is the reduced effective mass given by

$$\frac{1}{\mu^*} = \frac{1}{m_v^*} + \frac{1}{m_c^*}$$

The minimum energy separation of the bands as shown in Fig. 2(a) is denoted by E_g . There are several constant factors that appear in Eq. (2-4) which could be evaluated if the electronic wave functions were known. But, these are given throughout this chapter by one symbol whose numerical value is unimportant to the discussion. These constant factors will in general have different values for the different cases, but will not be given separate labels here. The first term in the matrix element of Eq. (2-5) will either be dominant or zero depending on whether the transition is "allowed" or "forbidden" by symmetry in the usual dipole sense. Assuming the matrix element to be constant in the neighborhood of $\vec{k}_c$ we find for the case of allowed transitions that

$$\alpha_a(E) = \frac{\text{const.}}{E}\left[E-E_g\right]^{1/2} \qquad (2\text{-}6)$$

and for forbidden transitions,

$$\alpha_f(E) = \frac{\text{const.}}{E}\left[E-E_g\right]^{3/2} \qquad (2\text{-}7)$$

These results neglect the Coulomb interaction between the electron in the conduction band and the hole in the valence band. It is possible that the bound electron-hole pair (exciton) can be excited to give large absorption values below the band gap and, similar to the absorption spectrum of hydrogen, there is absorption into the continuum which produces unbound electrons and holes. There is a comprehensive review article on excitons by Knox[25], and again, only the results are summarized here. As above we distinguish between the cases of allowed and forbidden transitions. One finds that for $E \leqslant E_g$ the absorption coefficient is given by either

$$\alpha_a(E) = \frac{\text{const.}}{E} \frac{e^z}{\sinh z} \qquad (2\text{-}8)$$

or

$$\alpha_f(E) = \frac{\text{const.}}{E} \left(1 + \pi^2/z^2\right) \frac{e^z}{\sinh z} \qquad (2\text{-}9)$$

where

$$z = \pi \left[\frac{E_{ex}(0)}{E - E_g} \right]^{1/2}$$

and $E_{ex}(0) = \frac{m^* e^4}{2\hbar^2 \epsilon^2}$ is the binding energy of the exciton. These results agree with the case when exciton effects are ignored for $E \gg E_g$, but have non-zero values at $E = E_g$.

It should be noted that these results are almost solely dependant on the form assumed for the shape of the bands, but near the extrema, parabolic bands are a good

approximation. We have also neglected the effects of degeneracy and more than one equivalent band. It is difficult to treat these cases, but this may not be a serious limitation since higher order effects such spin-orbit splitting may remove some of the degeneracy.

4. Indirect Transitions

It is possible that the extrema in the conduction and valence bands do not occur at the same point in $\vec{k}$ - space. From the considerations above one would not expect to observe absorption at energies below the minimum vertical energy separation of the bands because of the conservation of momentum. It is possible, however, that the lattice can give up or absorb the momentum required to make an indirect transition. Phonons or crystal defects may be sources or sinks for the momentum. These sources will provide only a small amount of energy for the transition, and the photon will still have to provide most of this energy.

The theory for indirect transitions is developed in a manner similar to that for direct transitions except that the interaction of the electron and hole with the lattice is taken into account. The details of the calculation become involved rapidly and are readily available elsewhere[23,24], so only the results are presented here.

Assuming that the bands in the neighborhood of the extrema are parabolic, and neglecting the effects of excitons, one finds that

$$\alpha_a(E)=\frac{\text{Const.}}{E}\sum_{\substack{\text{allowed}\\ \text{phonon}\\ \text{branches}}}\frac{1}{k\theta_i[\vec{k}]}\left\{\frac{|M'_{ie}|^2}{1-\exp\left(-\frac{\theta_i[\vec{k}]}{T}\right)}\left[E-\left(E'_g+k\theta_i[\vec{k}]\right)\right]^2\right.$$
$$\left.+\frac{|M'_{ia}|^2}{\exp\left(\frac{\theta_i[\vec{k}]}{T}\right)-1}\left[E-\left(E'_g-k\theta_i[\vec{k}]\right)\right]^2\right\} \qquad (2\text{-}10)$$

where k is Boltzman's constant, $\theta_i[\vec{k}]$ is the temperature associated with a phonon in branch i of the phonon spectrum, and E'_g is the indirect band gap energy as shown in Fig. 2(b). The first term under the summation corresponds to the absorption of a photon and the emission of a phonon, while the second term is associated with the absorption of a phonon and a photon. Each term will contribute to the absorption coefficient only when the squared quantity is positive. The exponential factors give the number of phonons which can be absorbed or emitted by the lattice at the temperature T. As above it is necessary to differentiate between allowed and forbidden transitions. Equation (2-10) is changed by summing over the forbidden branches of the phonon spectrum and allowing the absorption to rise as $(\Delta E)^3$. The temperature dependance in the two cases will be the same.

The problem rapidly increases in complexity when the effects of excitons are included. For photon energies near the band gap, the absorption spectrum can generally be described by the relation

$$\alpha(E)=\frac{\text{Const.}}{E}\sum_i \left\{ \frac{|M''_{ic}|^2}{1-\exp\left(-\frac{\theta_i[\vec{k}]}{T}\right)} F_i\left[E-(E_g'-E_{ex}(0)+k\theta_i[\vec{k}])\right] \right. \tag{2-11}$$

$$\left. + \frac{|M''_{ia}|^2}{\exp\left(\frac{\theta_i[\vec{k}]}{T}\right)-1} F_i\left[E-(E_g'-E_{ex}(0)-k\theta_i)\right] \right\}$$

where the functional form of $F_i[E]$ depends on whether the transitions are allowed or forbidden. There are a series of contributions beginning at the onset of transitions into the lowest exciton state and rising until there are transitions producing unbound electron-hole pairs. For allowed transitions, the absorption coefficient rises initially as the $1/2$ power, and then rising as the $3/2$ power, eventually going to a squared dependance. For forbidden transitions, the series $3/2$, $5/2$, 3 should be observed. This equation describes the creation of an "indirect" exciton from a hole near $\vec{k}_v$ (the valence band wave vector) and an electron near $\vec{k}_c$ (the conduction band wave vector). This is opposed to the "direct" exciton whose electron and hole wave vectors are nearly the same. The two terms under the summation correspond to the creation of an exciton and a phonon, and the creation of an exciton and annihilation of a phonon by

photons respectively. This is similar to the case of indirect band to band transitions that create unbound electrons and holes.

To summarize, the simple theory predicts that near the onset of transitions, the absorption will rise as a function of the photon energy minus a constant to some power. For direct transitions, the theory predicts there will be a smooth rise in the absorption proportional to $(\Delta E)^{1/2}$ or $(\Delta E)^{3/2}$ depending on the symmetry. For indirect transitions, there will be several components which will give, not a smooth curve, but one with "knees" or "bumps" in it corresponding to the onset of phonon emission or absorption. A careful analysis of the absorption edge spectrum should indicate whether the band gap is direct or indirect, and give the value of the exciton binding energy and the value of the band gap. The methods used to analyze the experimental data to get this information will be presented in Chapter IV.

CHAPTER III

EXPERIMENTAL TECHNIQUES

1. Determination of the Absorption Coefficient

Measurement of the intensity of light entering and leaving a sample of thickness d may be used to measure the absorption coefficient since both the intensity and energy are proportional to $\langle \vec{\mathcal{E}} \rangle^2$. Phenomenologically, the absorption coefficient is defined by the relation

$$I_T = I_o' \, e^{-\alpha d}$$

where I_T is the intensity transmitted by the sample and I_o' is the intensity just inside the first surface. Some of the light entering the sample is reflected and must be taken into account in any real measurement. Let I_o be the true incident intensity and R the ratio of the intensity reflected from the air-sample interface, then

$$\frac{I_T}{I_o} = \frac{(1-R)^2 \, e^{-\alpha d}}{1 - R^2 e^{-2\alpha d}} \qquad (3\text{-}1)$$

is the correct expression for the transmittance of a sample in air neglecting any interference effects.

The absorption coefficient may be determined from values of R and the transmittance. The reflectance R, however, is difficult to measure at normal incidence.

To a very good approximation, the reflectance need not be known if the transmittances of two samples of thickness $d_1 \neq d_2$ are measured. The ratio of the transmittances T_1 and T_2 is

$$\frac{T_1}{T_2} = e^{-\alpha(d_1-d_2)} \left[\frac{1-R^2e^{-2\alpha d_2}}{1-R^2e^{-2\alpha d_1}} \right] \qquad (3\text{-}2)$$

The quantity in brackets will be nearly unity when $R^2e^{-2\alpha d} \ll 1$. Therefore Eq. (3-2) may be used to measure α. This technique has been used consistently to measure the absorption coefficient.

The apparatus used to measure the transmittances is shown schematically in Fig. 3. The tungsten filament source (S) was water colled and operated from a battery (B) to give the needed stability. Mirrors M_1 and M_2 focused the filament on the entrance slit (E) of a Leiss double prism monochromator equipped with flint glass prisms to give high dispersion in the visible portion of the spectrum. The monochromatic light from the exit slit (E') was refocused in the cryostat (C) by the mirrors M_3 and M_4. Either of the two samples S_1 and S_2 may be rotated into the beam. The intensity of the transmitted light was detected by an EMI 9558QA 10-stage photomultiplier tube (P) which has an S-20 spectral response for low dark current and high quantum efficiency near 7000Å. The high voltage for the photo tube was provided by a

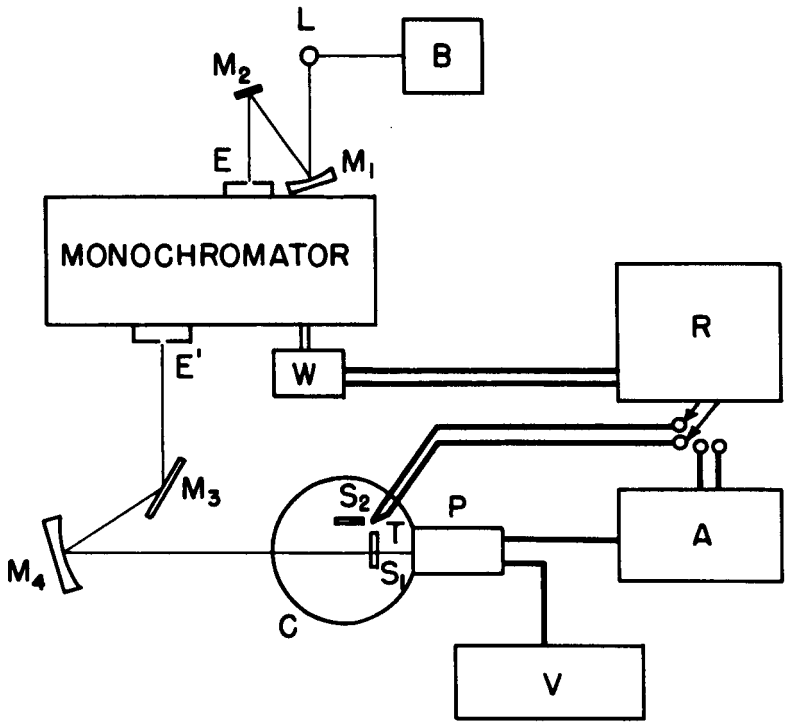

Fig. 3. Schematic diagram of experimental apparatus

Fluke 403M d-c supply (V), and the current was measured by a Keithley 414 micro-microammeter (A). The output of the ammeter was fed into a Minneapolis Honeywell (Brown) recorder (R) equipped with an operation pen which was coupled to the wavelength drive (W) so that photo-current and wavelength could be recorded simultaneously. The sample temperature was measured by a thermocouple (Au: 2.1%Co-Ag: 0.37%Au) (T).

The monochromator was calibrated against the operation pen markers using spectral line sources. The calibration is accurate to $\pm$ 0.001 eV and the instrument was capable of resolving $\sim$0.0005 eV in the region of interest. The intensity of the lamp was constant at all wavelengths after a 15 minute warm-up time and only freshly charged batteries were used for each set of measurements. The photocurrent was recorded continuously as a function of the wavelength for both samples, one after the other, always scanning in the same direction to minimize the effects of backlash in the monochromator. No difference in the results was observed when the order of the measurement was reversed. The cryostat consisted of a liquid air reservoir which was isolated from the samples. Cooling to any temperature between liquid helium temperature and room temperature was achieved by circulating the liquid from the reservoir around the sample

holder. An outer liquid nitrogen shield kept radiation losses small, and the sample was surrounded by a second shield which was kept at the same temperature as the sample. The thermocouple used to measure the sample temperature was mounted on the sample holder since the thin samples would not support a thermocouple junction. No difference in temperature could be detected between the sample holder and a thick sample itself at 80°K. The temperature measurements are believed to be accurate and constant throughout the time of measurement to $\pm 3^{\circ}K$ at all temperatures. All samples were maintained at the desired temperature for more than 30 minutes before measuring to be certain that thermal equilibrium had been reached.

The absorption coefficient was determined from the relation

$$\alpha = \frac{\ln_e (i_1/i_2)}{d_2 - d_1}$$

where i_1 and i_2 are the photocurrents corresponding to the two transmittances. The thicknesses d_1 and d_2 were measured using micrometer calipers which gave an uncertainty in the thickness of $\pm 3\mu$, but the observed deviations were considerably less. Thin films were checked using the Fizeau interferometric method[26] and $\pm 1\mu$ accuracy was demonstrated. The estimated error in the absorption coefficient is about $\pm 1\%$, or ± 0.03 cm^{-1} at low levels.

The sample holder in the cryostat was a massive piece of copper with recessed holes in which the samples could be held with copper retaining rings. It was necessary to use thin Kel-F[27] rings on either side of the sample to prevent breaking the samples at low temperatures.

2. Sample Preparation

Two techniques were used to prepare samples for absorption measurements. First, amorphous samples were made by rapid cooling from the molten state, and second, vacuum evaporation was used. To insure that the samples were amorphous, Laue diffraction patterns were observed which showed no apparent order. The selenium used in this study was purchased from the American Smelting and Refining Company. The purity was believed to be greater than 99.999% with less than 1 ppm. of: Te, Cu, As, Si, S, and other halogens. Further purification was not attempted.

No special techniques are required to handle molten selenium because of the low melting point (217°C). Samples without bubbles or other defects were prepared by melting the selenium in an evacuated, sealed pyrex tube 1 cm in diameter. The melt was maintained at 360°C for several hours and cooled by immersion in 20°C water. The time required to cool the selenium was less than 5 seconds. After removing the glass tubing, the selenium was cut with a diamond saw into 2 mm thick pieces which were mechan-

ically polished using aluminum oxide grit with soapy water as the lubricant. The minimum sample thickness which could be obtained in this manner was about 0.5 mm. The samples were examined at liquid nitrogen temperature for hidden defects using a low power microscope.

Considerably thinner samples could be prepared by vacuum evaporation. There was severe damage to the films evaporated on quartz or pyrex substrates when cooled below $0^{\circ}C$ because of mismatched thermal expansion coefficients. The films would adhere to either sodium chloride or Kel-F[27] substrates at all temperatures because their thermal expansion coefficients more closely match that of selenium. In order to remove all stress on the film caused by the substrate, selenium was evaporated onto aluminum coated Mylar substrates[28] which were 0.001 in. thick. The necessity of unsupported films is demonstrated in the following chapter.

The Mylar could be peeled away from the selenium leaving an unsupported film. All evaporations were done at a pressure of $\sim 10^{-5}$ torr keeping the crucible at $360 \pm 5^{\circ}C$ and the substrate at $52 \pm 2^{\circ}C$. The substrates were located approximately 5 inches from the crucible which gave an evaporation rate of about 2.5Å per minute. The substrate holder was designed to permit two films of different thicknesses to be evaporated under identical

conditions. To insure that the temperature would be uniform across the thin substrate, it was necessary to mount the mylar sheets on more massive pieces of glass using Corning vacuum grease as the binding agent. The completed films were removed from the vacuum chamber immediately after evaporation, the mylar was slid off the glass, and peeled away from the selenium film. This process and mounting the film in the cryostat took no more than ten minutes. The procedure prevented curling of the films and kept contaminants from the air at a minimum. Unsupported films as thin as 10 μ could be produced in this way.

CHAPTER IV

RESULTS

1. General Observations

The absorption edge of amorphous selenium has been studied by many workers. A large amount of this work has been done at room temperature. Previous results[11-12,29-33] and the values found in this study have been summarized in Fig. 4. The collection of data covers a time span of about 15 years, and many different sources of selenium, methods of sample preparation, and techniques of measurement are represented. In spite of these differences, the agreement is remarkably good. The purpose of the present study was not simply to add to the fund of data shown in Fig. 4, but to examine the lower portion of the curve more closely in an effort to determine the functional dependance of the absorption on energy and temperature and to get some insight into the absorption process.

One feature of the absorption spectrum which is immediately apparent is that α appears to vary exponentially with photon energy over many orders of magnitude. The discussion in Chapter II would lead one to expect such a dependance if the simple band model and density of states were applicable in this case. Since the equations given above are valid only for

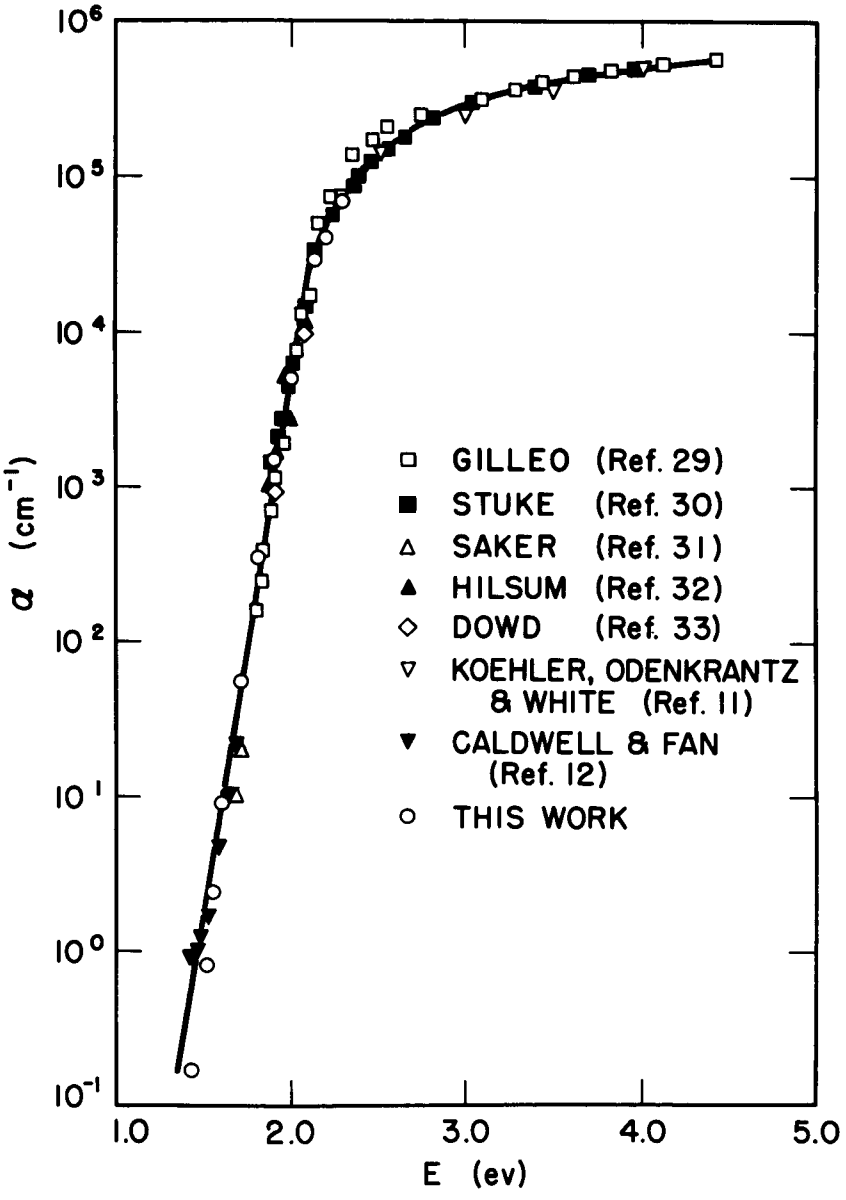

Fig. 4. The absorption-edge spectrum of amorphous Se at room temperature

photon energies near the band gap, a close examination of the low energy tail of the spectrum at many temperatures is necessary to reveal the structure predicted by the band model.

The temperature dependance of the absorption edge was measured by Gilleo[29] in 1951. He observed that at relatively low absorption values, the edge shifted towards higher energies with decreasing temperatures. In Fig. 5 of his paper, he has plotted the logarithm of α against $1/T$ for eight wavelengths. The absorption spectrum Gilleo observed at three different temperatures has been replotted from that data here in Fig. 5 to show the shape of the absorption spectrum more clearly. The exponential behavior appears to hold even to the lowest temperature he measured, but the small number of points for each curve makes a detailed analysis difficult. The change of the slope with temperature in Gilleo's data was noted by R. M. Blakney[34] and compared to Urbach's empirical rule[35] first observed in the absorption spectrum of the silver halides in 1953:

$$\alpha = \alpha_o \exp\left[\sigma/kT\,(E - E_o)\right] \qquad (4\text{-}1)$$

where α_o, σ and E_o are constants characteristic of the material, and T is measured on the absolute scale. Using Gilleo's data, Blakney found the value of σ to

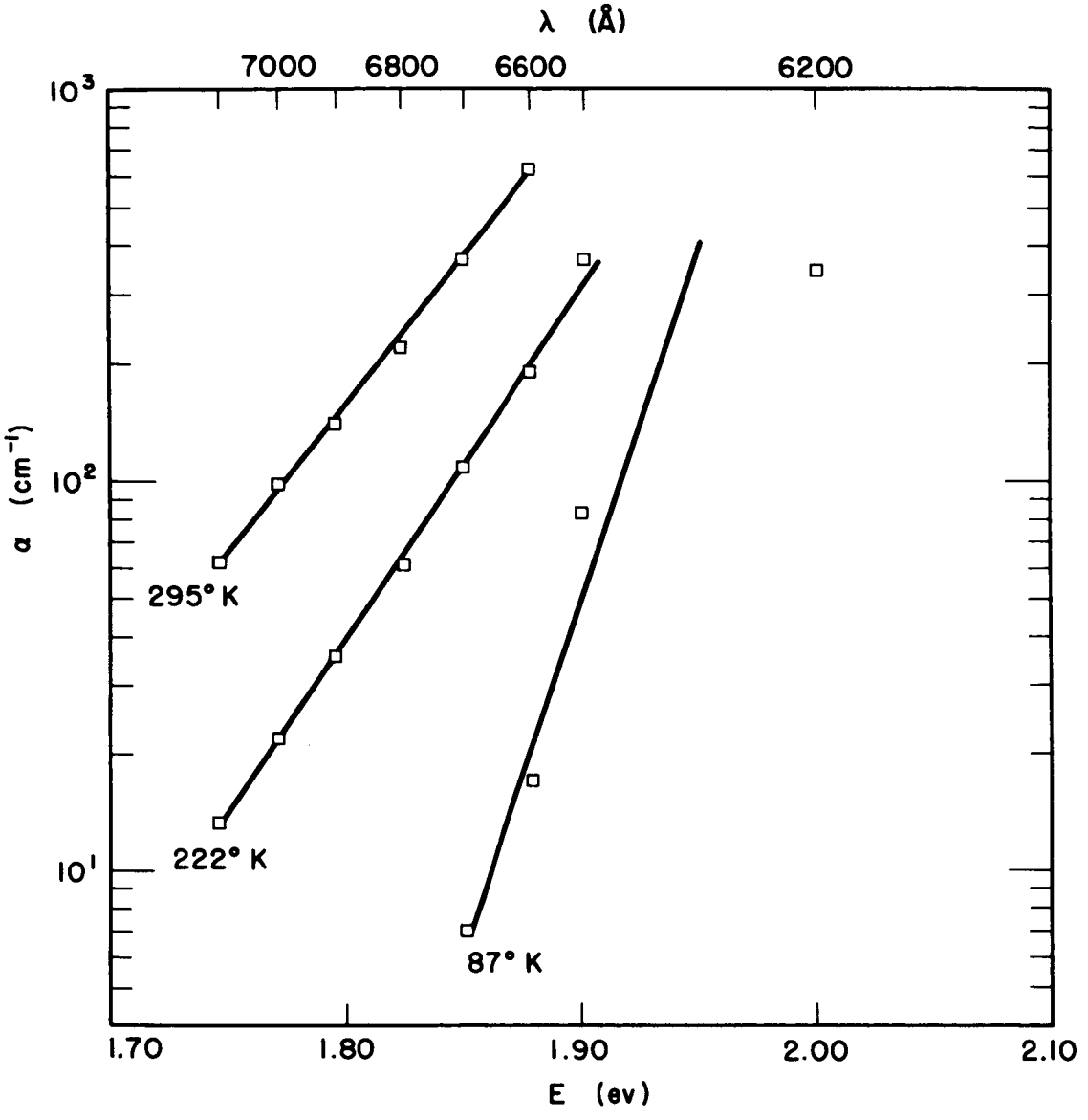

Fig. 5. A portion of the absorption edge of amorphous Se at 295°K, 222°K, and 87°K (after Gilleo, Ref. 29)

have a nearly constant value of 0.4, but the magnitude of the shift was not consistant with Eq. (4-1). This is not too surprising since the rule had previously been reported only for crystalline materials. In order to study the apparent close connection between Urbach's rule and Gilleo's data, a more detailed study of the absorption edge in this region has been made. The values of the absorption coefficient measured in this investigation have been plotted in Fig. 6 for nearly the same three temperatures shown for Gilleo's data in Fig. 5. The two sets of data shown are for unsupported films and films evaporated onto freshly polished sodium chloride substrates. The rate of evaporation and substrate temperature during evaporation were identical for the two sets of films. The apparent difference in the values of the absorption coefficient for the supported and unsupported films is due to the effect of substrates. Since the curves at room temperature agree fairly well, it is possible that the difference in the coefficients of expansion of the two materials intorduces a large amount of strain into the sample on the substrate, especially at low temperatures. The discrepancy between the measured values of α for this study and Gilleo's[29] is even larger. The slope of the exponential at room temperature is about the same for both cases, but Gilleo's results are about

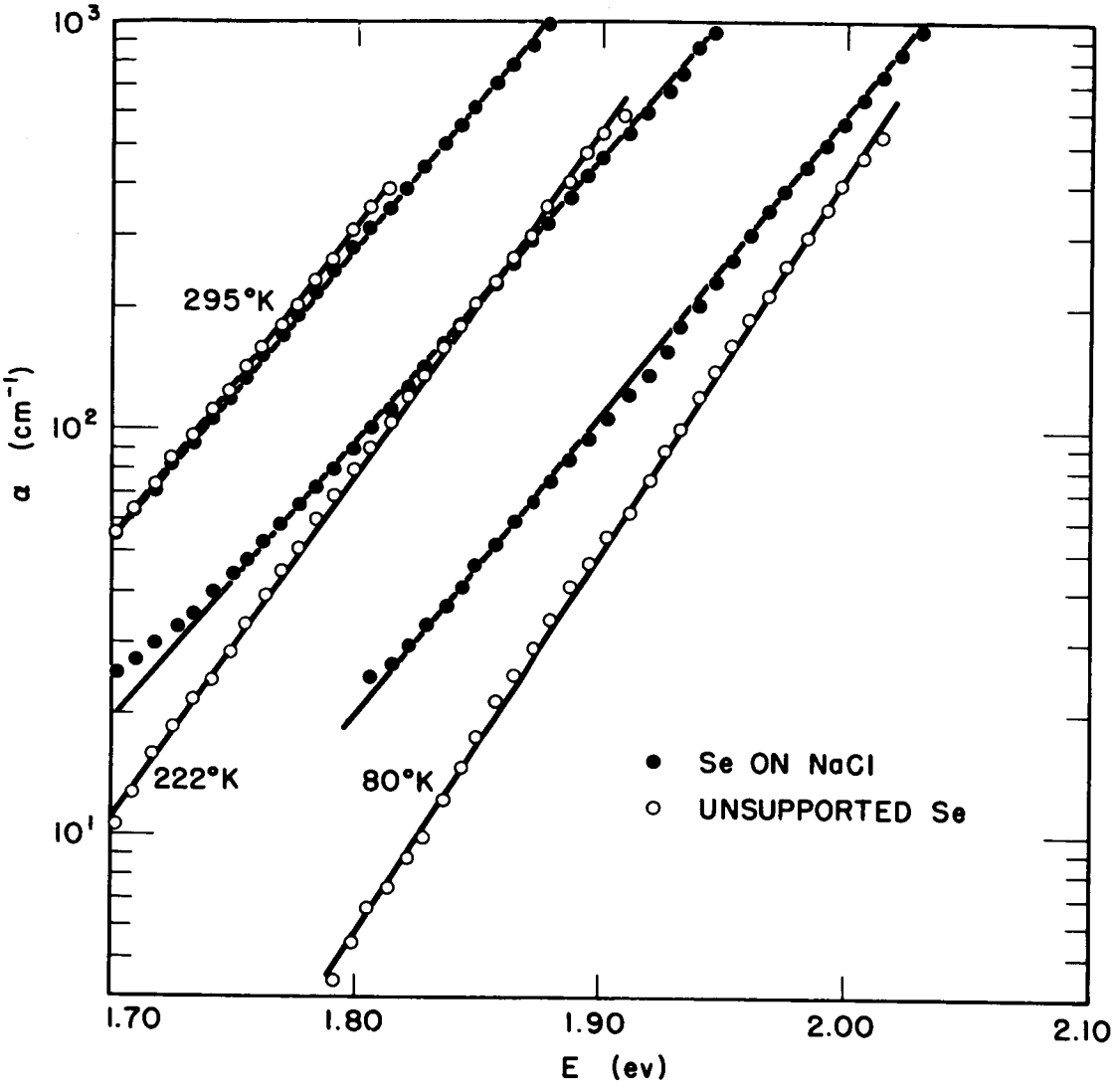

Fig. 6. The absorption edge of amorphous Se films with and without substrates

a factor of 2 larger than the values of Fig. 6. Two different techniques were used to measure the film thickness in the two studies which could, in part account for the difference. Another large difference between these results is the change in slope which Gilleo observed which was never seen to such a degree in the present study. The electrical properties of evaporated selenium films have been shown to depend on the temperature of the substrate during evaporation[36]. The optical properties might also show such a dependance which would help to account for some of the discrepancies in the results of the two studies. Since Gilleo did not report the substrate temperature used for his experiment, nothing definite may be said about this either. Whether Gilleo's "rock salt" substrates were cleaved or polished is likewise not known. The cleaved surface might have an effect on the bonding and hence strain introduced at low temperatures.

The shift of the absorption coefficient with temperature is often discussed in terms of the lattice dilation effect and the lattice broadening effect[10]. The results of this measurement for these three different sets of data are shown in Fig. 7 where the energy for which $\alpha = 23.5\ cm^{-1}$ is plotted against absolute temperature. The slopes of the linear portions are indicated

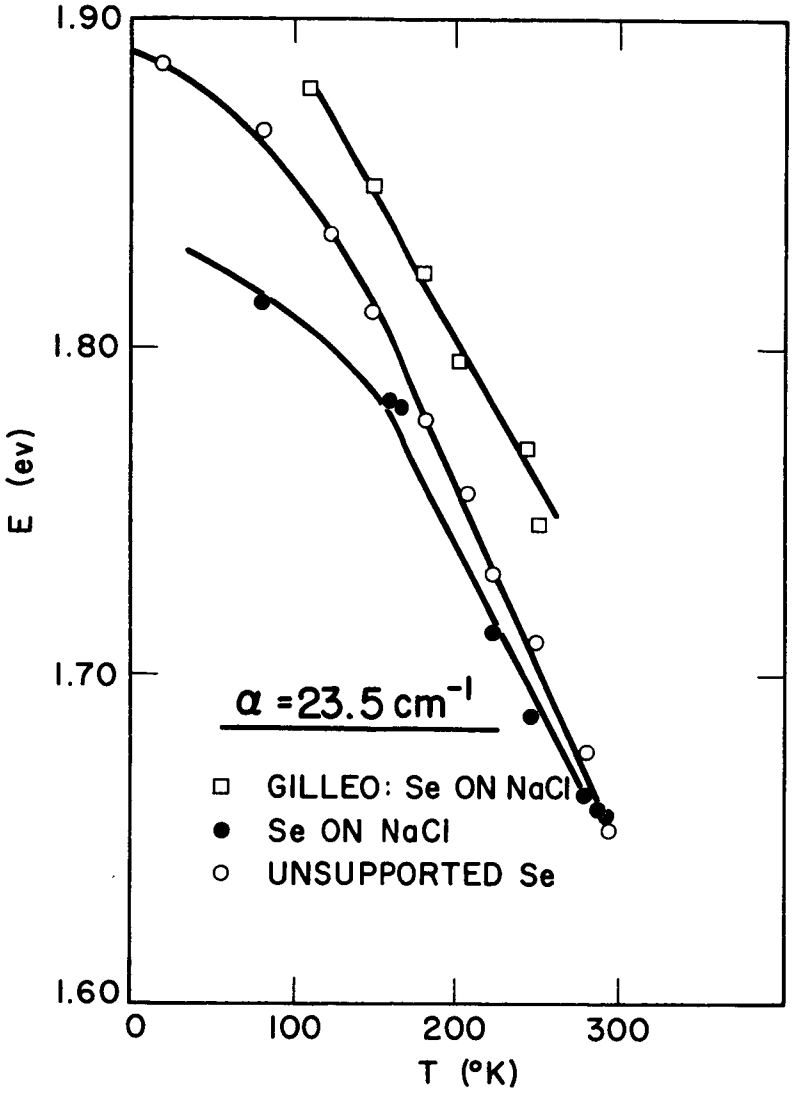

Fig 7. Temperature dependence of the absorption edge

in the figure. The unsupported films seem to show a larger shift, but in general, these results are in reasonable agreement, with values near 10^{-3} eV/°K.

2. Investigation of Structure in the Absorption Edge

Because of the large effect of the substrates on the optical absorption edge, only the results for unsupported films will be discussed further in hopes that the data are representative of the material itself. The slight deviations from the exponential edge seen upon close inspection of data for unsupported films in Fig 6 will be the subject of all further discussion.

The absorption edge of hexagonal selenium was investigated by Choyke and Patrick[37] using a photovoltaic method from which only the relative absorption may be deduced. A more recent measurement on single selenium crystals by Eckart and Henrion[38] used direct optical methods. Both studies found that the onset of absorption was characteristic of indirect band to band transitions. Because of the close relationship which exists between hexagonal and amorphous selenium, the results of the former study are presented here for comparison. The square root of the relative absorption coefficient has been plotted against photon energy for Chyoke and Patrick's data[37] in Fig. 8(a). Both their experimental data and the curves generated from the expression

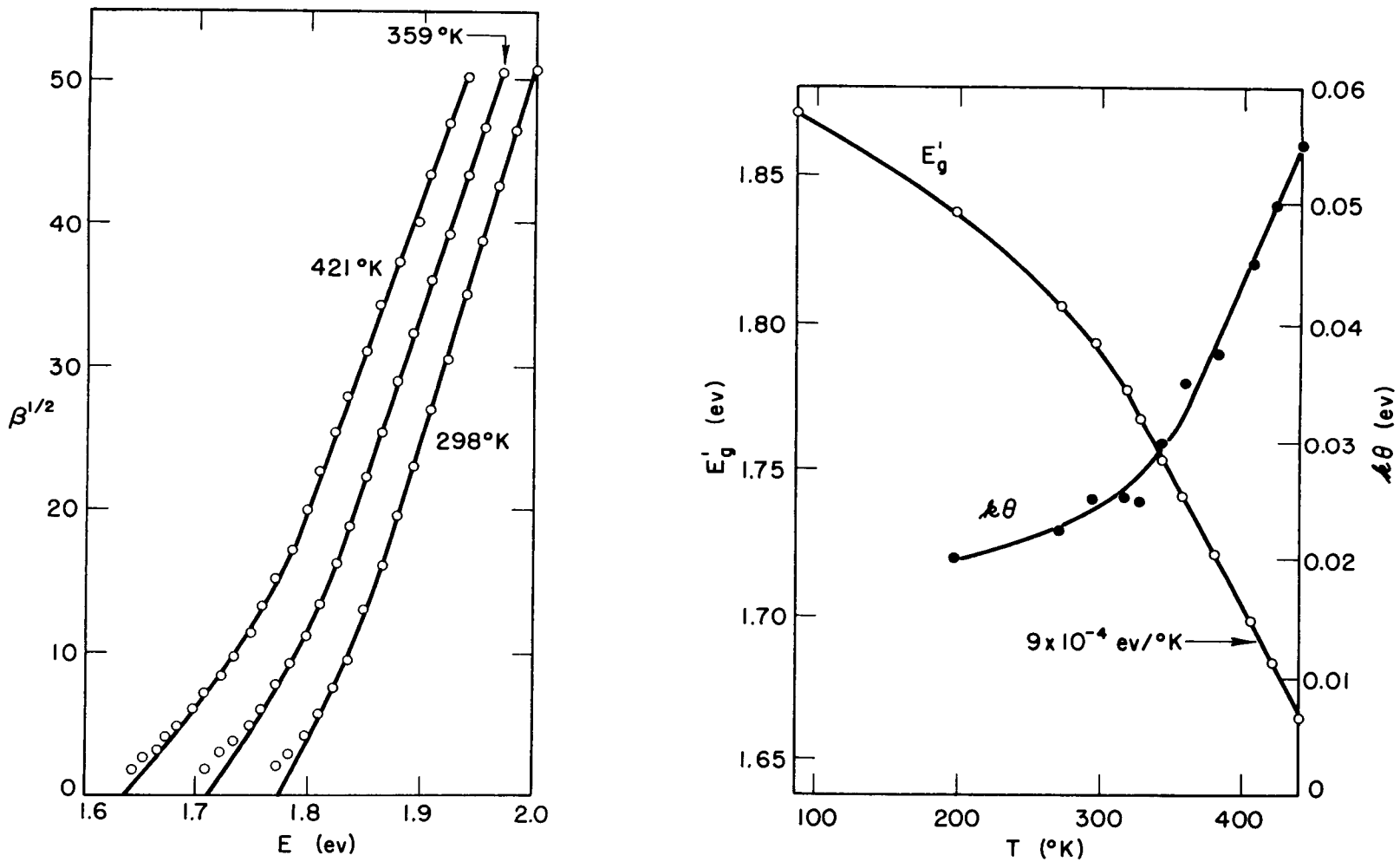

Fig. 8. (a) Relative absorption of hexagonal Se (b) Temperature dependence of E_g' and $\hbar\theta$ (after Choyke and Patrick, Ref. 37)

$$\beta = 3X10^{+4}\left[\frac{(E-E_g'+k\theta)^2}{e^{\theta/T}-1} + \frac{(E-E_g'-k\theta)^2}{e^{\theta/T}-1}\right]$$

are shown. The values of the indirect band gap and the phonon energy they have deduced from the experimental data are shown in Fig. 8(b). These results are indicative of indirect band to band transitions similar to the early work on germanium and silicon[39,40]. The strongly temperature dependant phonon energy which they needed to fit the data is somewhat unusual, however. They have argued that since the crystalline form expands along the c-axis and contracts perpendicular to the c-axis on cooling, the unusual temperature dependance of the phonon energy is not surprising. They experienced considerable difficulty at lower temperature in fitting the data as indicated by the missing points below 200°K in Fig. 8(b) for the phonon energy. Eckart and Henrion[38] measured the spectrum only at room temperature, but found that $k\theta = 0.06eV$ and for light polarized parallel and perpendicular to the c-axis $E_{g\parallel}' = 1.76\,eV$ and $E_{g\perp}' = 1.73eV$ respectively.

In the present work, the low energy tail of the absorption spectrum of amorphous selenium was closely analyzed to see if there was any similarity between it and the spectra measured by others for hexagonal selenium. First attempts were made to fit the experimental data to an expression of the form

$$\alpha = C_1 (E-E_1)^2 + C_2 (E-E_2)^2 \qquad (4\text{-}2)$$

where C_i and E_i are parameters which are dependant only on the sample temperature. A computer program described in the Appendix was used to determine the values of C_i and E_i which would give the best fit. The phonon energy and the indirect band gap energy were determined from the relations

$$k\theta = \tfrac{1}{2}(E_2 - E_1)$$

and

$$E_g' = E_2 - k\theta$$

where $E_2 > E_1$. The value of M in Eq. (2-10) could be determined numerically from C_1, C_2 and θ. According to the theory, M should be independant of the sample temperature, but a strong temperature dependance was needed in the term corresponding to phonon absorption in order to agree with the data. Rather than impose some arbitrary temperature dependance on M it was found that adding a constant term $S(\theta)$ to the expression for the number of phonons which could be absorbed at a temperature T allowed the data to be fit in a convincing manner. The constant $S(\theta)$ corresponds to a source of momentum for the indirect transitions which is independant of temperature. This takes into account the way in which defects can act as sources of momentum in a perfect crystal. It is not

surprising to find such a term in amorphous selenium where the "defects" will be so prevalent. The proposed equation for the absorption coefficient when there are other sources of momentum in addition to phonons is given by

$$\alpha = M\left\{\left[S(\theta)+\frac{1}{e^{\theta/T}-1}\right]\left[E-(E_g'+k\theta)\right]^2 + \frac{1}{1-e^{-\theta/T}}\left[E-(E_g'-k\theta)\right]^2\right\} \quad (4\text{-}3)$$

The experimental data and the curve generated from this expression are shown in Fig. 9 where the values of E_g' and $k\theta$ shown in Fig. 10 were used to calculate the solid curves with $S(\theta) = 0.0925$ and $M = 10^4$ eV^{-2} cm^{-1}, in Eq. (4-3).

The agreement between the shape of the experimental data and the computed curves, while not perfect, is surprisingly good. The temperature dependance of the indirect band gap and phonon energy show some similarity to that seen in Fig. 8(b). The phonon energy is larger than that measured in the same temperature range by Choyke and Patrick[37], but agrees with the results of Eckart and Henrion[38]. The infrared absorption spectrum of amorphous selenium shows maxima at 0.0314 eV and 0.0608 eV. The latter showing a temperature shift[41] identical to that observed here.

There is one feature of the curves shown in Fig. 9 which is present at all temperatures. At the knee of the

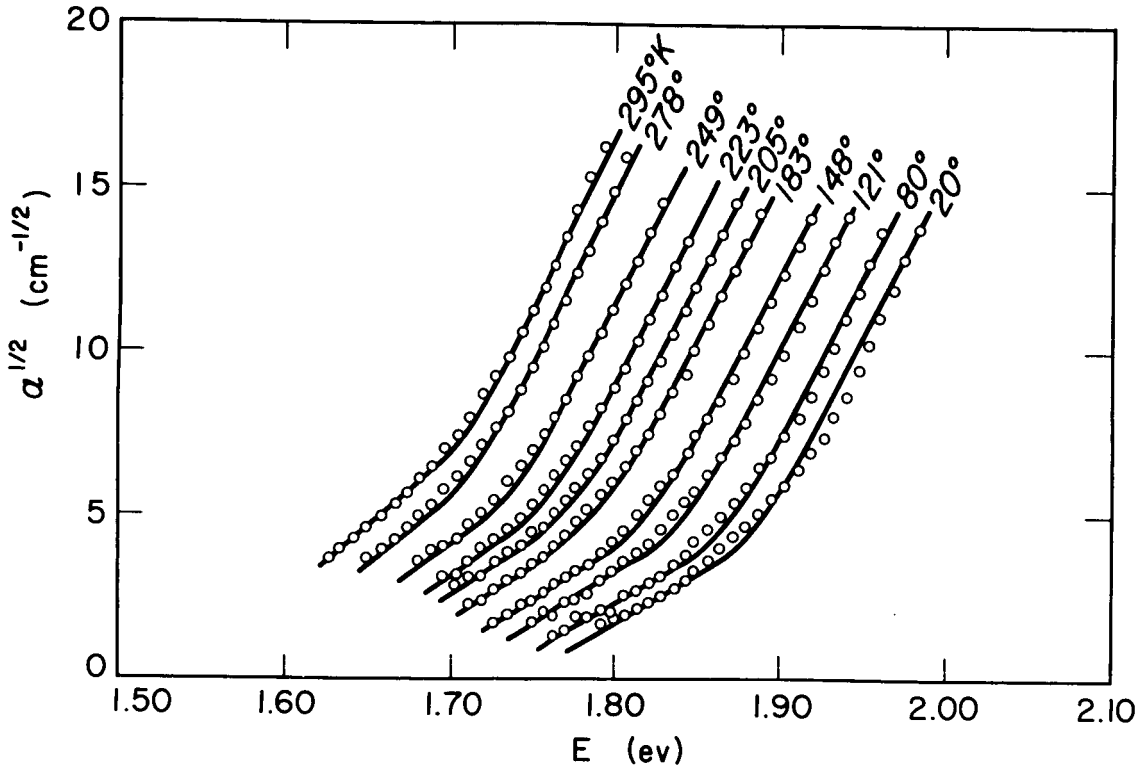

Fig. 9. Absorption edge of amorphous Se indicating indirect transitions

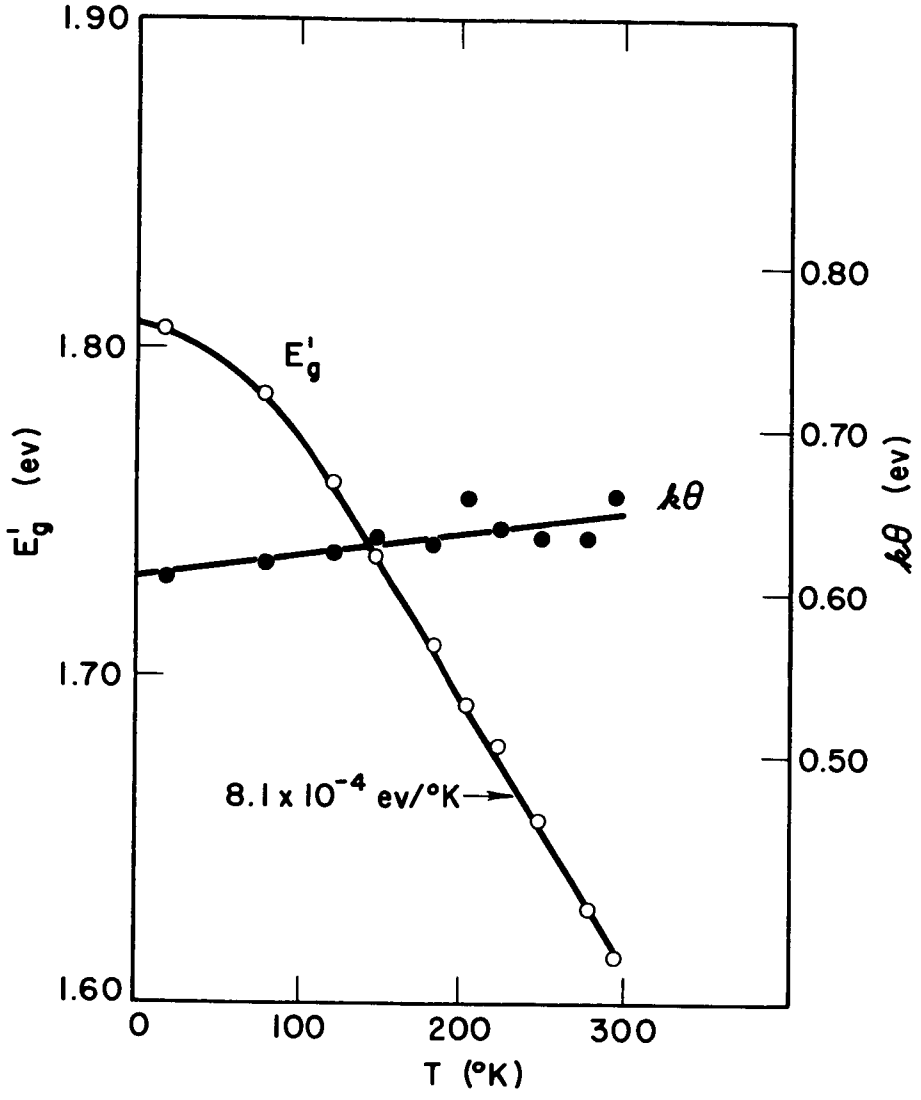

Fig. 10. Temperature dependence of E'_g and $k\theta$ for amorphous Se

curves between the two nearly linear portions a small, sudden rise in the absorption is seen which is similar, although less pronounced, to a feature in the germanium spectrum that has been interpreted as absorption by excitons[1]. An exciton level has been proposed for amorphous selenium which lies 0.08 eV below the conduction band[23]. The discussion in Chapter II showed that the behavior of the absorption coefficient becomes more complex when indirect excitons are included. The problem of fitting the data is an extension of the case described above except that we now need to fit the expression

$$\alpha = \sum_i C_{ei} (E - E_{ei})^{3/2} + \sum_j C_{bj} (E - E_{bj})^2 \qquad (4\text{-}5)$$

to the experimental data. The first summation describes formation of indirect excitons and the second accounts for band to band transitions. The data shown previously in Fig. 9 has been repeated in Fig. 11 where curves for only four temperatures are shown. The solid curve was calculated from Eq. (4-5) using the value of C_i and E_i which gave the best fit. The two lowest temperature curves were fit with four terms in Eq. (4-5), two of each power. The best fit for the two highest temperature curves was obtained only when three 3/2 power terms and two squared

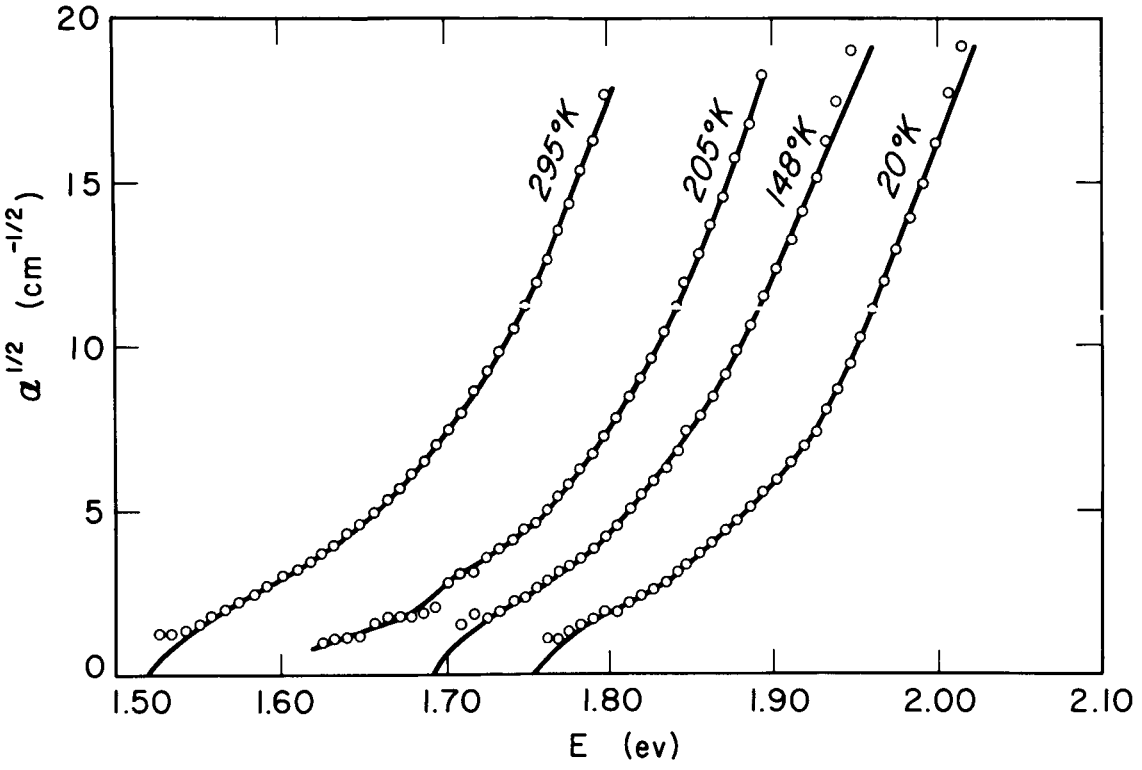

Fig. 11. Absorption edge of amorphous Se showing the effect of excitons

terms were used. The addition of this term may correspond to the formation of excitons with higher energy phonons, but the evidence for this is too slight to be able to form any definite conclusions. The values of E_g', $E_{ex}(0)$ and $k\theta$ were determined from the fitted curves using the relations

$$k\theta = \tfrac{1}{2}(E_{b2} - E_{b1}),$$

$$E_g' = E_{b2} - k\theta$$

and

$$E_{ex}(0) = E_g' + k\theta - E_{c3}$$

The values of these quantities which gave the best fit are given in Table I, and the temperature dependance of the indirect band gap is indicated in Fig. 12. The value of $k\theta$ should also be given by $\tfrac{1}{2}(E_{c3} - E_{c2})$ but it was believed that small errors in the measurements of the low values of the absorption coefficient rendered the values calculated in this manner less accurate. The fact that there was good agreement at room temperature was thought to indicate that the same energy phonon was responsible for both the indirect band to band transitions and the formation if indirect excitons. It is seen on inspection of Table 1 that the value of $E_{ex}(0)$ has an average value of 0.076 eV which is in good agreement with the value found by Hartke and Regensburger[23]. This energy is probably independant of temperature over the

T(°K)	E_{e1}	E_{e2}	E_{e3}	E_{b1}	E_{b2}	$k\theta$	E_g'	$E_{ex}(0)$
20	-----	1.755	1.832	1.872	1.916	0.022	1.894	0.084
148	-----	1.692	1.781	1.795	1.849	0.027	1.822	0.068
205	1.592	1.671	1.751	1.783	1.824	0.020	1.803	0.072
295	1.521	1.613	1.660	1.695	1.739	0.022	1.717	0.079

Table 1 Measured values of E_{ei} and E_{bi} and the calculated values of $k\theta$, E_g' and $E_{ex}(0)$.
All energies are given in electron volts.

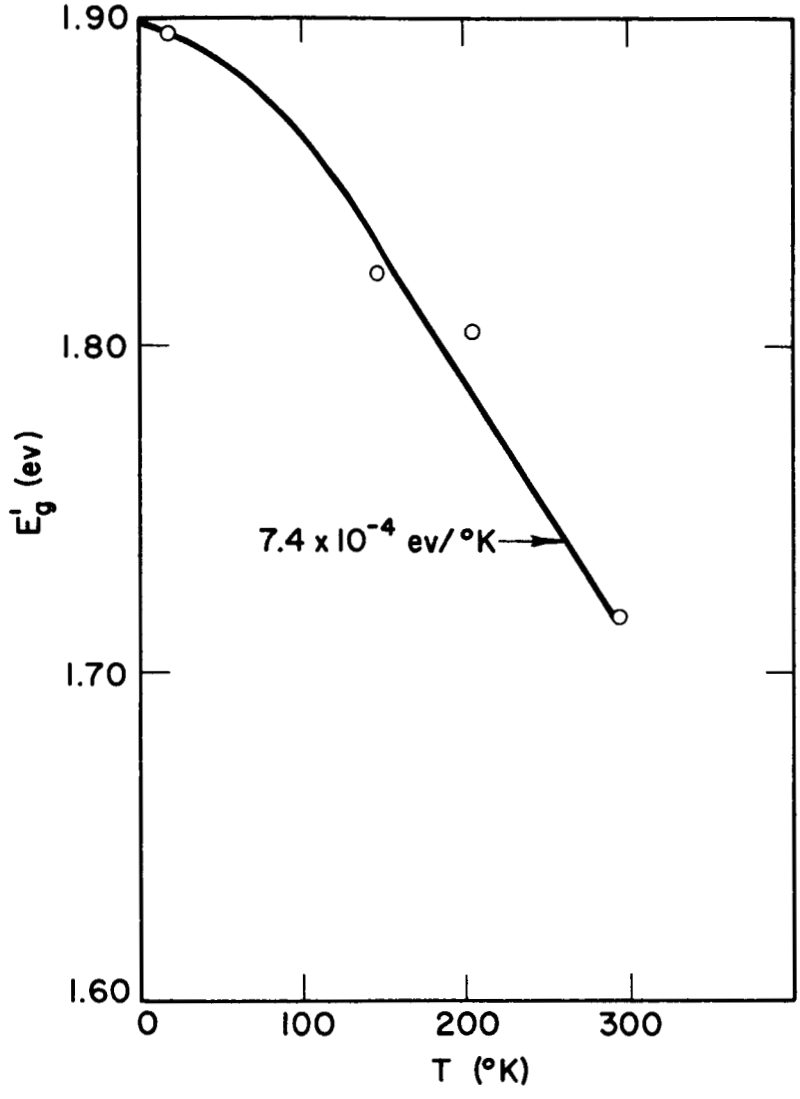

Fig. 12. Temperature dependence of the indirect band gap

range of these measurements. Another satisfying result is that the phonon energy has now been shown to have a nearly constant value of 0.023 eV which is a more reasonable energy than when exciton effects are omitted.

The effect of errors in the low absorption measurements also seems to have shown up in the coefficients C_{ei} and C_{bi} given in Table 2. Although there are some slight inconsistancies, the portion of the curve corresponding to indirect band to band transitions can be described by an expression of the form of Eq. (4-3) letting $S(\theta) = 0.305$ and $M = 1.08 \times 10^{4}$ eV^{-2} cm^{-1}. The remainder of the curve describing the creation of indirect excitons could not be described by such a simple extension of the theory of Chapter II. Although the coefficients have the proper tendency to increase with increasing temperature, no strict functional dependance on temperature was observed. One possible reason for this is that the coefficients calculated are very sensitive to small errors. These errors will probably not affect the functional dependance on photon energy, but will tend to obscure the exact temperature dependance of these coefficients. It is also possible that the mechanism for the formation of indirect excitons in an amorphous solid is not properly represented in the simple theory for crystalline solids.

These details of the lack of correspondance between the coefficients of the energy terms found in the exper-

T(°K)	C_{e1} $eV^{-3/2}cm^{-1}$	C_{e2} $eV^{-3/2}cm^{-1}$	C_{e3} $eV^{-3/2}cm^{-1}$	C_{b1} $eV^{-2}cm^{-1}$	Cb_2 $eV^{-2}cm^{-1}$
20	----	333.	729.	3290.	16700.
148	----	452.	953.	3340.	11300.
205	136.	513.	1560.	7310.	14200.
295	391.	523.	1380.	7240.	11500.

Table 2 Measured values of C_{ei} and C_{bi}.

imental data and that proposed by the simple theory is not thought to be a serious limitation considering that the theory of indirect transitions has been developed for perfect crystals, not amorphous solids. Judging from the results shown in Fig. 11, it is the conclusion of this study that the tail of the absorption edge in amorphous selenium is caused by indirect transitions between the conduction band and the valence band, and by the formation of indirect excitons. The deviations between the calculated curve and the experimental data at low absorption values are probably due either to small errors in the measurement or to absorption by impurity or defect states that must exist because of the disorder. The continued rise in the measured absorption at the higher levels is undoubtedly due to other transitions which may be direct, although the difficulty encountered in making and measuring thinner unsupported films prevented an investigation of this conjecture.

CHAPTER V

DISCUSSION

Although optical absorption near the fundamental absorption edge of semiconductors is capable of predicting the shape and location of the highest valence band and the lowest conduction band, in practice, such predictions are difficult. The experimentalist must keep a careful eye toward progress in theoretical calculations and results of other experiments. In this chapter a tentative extension of an existing band calculation is made with the realization that the data found above are insufficient to make any definite determination of the bands. The proposed energy band model for amorphous selenium is believed to explain not only the optical properties, but many of the other experimental observations as well. To better understand the reasons behind the proposed extension, a review of previous band calculations on both selenium and related materials is presented together with a discussion of some pertinent experiments on the electrical properties of amorphous and hexagonal selenium.

Early work on the band structure in selenium is reviewed by Olechna and Knox[42] who have just completed a tight binding calculation for selenium chains. Since the major feature of the structure of amorphous selenium

is the long spiral chains, this calculation has been chosen as the starting place for modifications which will aid in explaining the observed properties. Their results, which will be discussed at greater length below, showed that along the direction of the chains (c-axis in hexagonal selenium). The minimum band gap is direct and located in $\vec{k}$ -space away from $\vec{k} = 0$. Herman has done a "nearly empty lattice" calculation for hexagonal selenium[43] which shows a minimum in the conduction band which would give rise to indirect transitions, but Knox[44] feels that the tight (nearly covalent) binding along the chains would rule out the possibility for such a band shape. Hulin[45] has done an L.C.A.O. calculation for tellurium whose structure and properties are similar to those of selenium. His calculation showed that the energy bands are similar to those found by Olechna and Knox in the same direction in $\vec{k}$ -space, but that the minimum separation in the bands occured at other points. The behavior of both the conduction and the valence bands was quite complex, and he was not able to state exactly where the extrema occured. We can conclude that theoretical studies have shown that along the direction of the chains the band gap is direct and that there may be a maximum in the valence band and a minimum in the conduction band somewhere else in $\vec{k}$-space.

For further clues into the form of the bands, let us review some of the recent experimental work which has been done on the photoelectrical properties of both hexagonal and amorphous selenium. Gilleo[29] measured the absorption edge and photoconduction edge for both hexagonal and amorphous selenium. He found that the absorption edge and the photoconduction edges in the hexagonal modification nearly coincided, but that the onset of photoconductivity in the amorphous material was shifted toward higher energies by about 0.3 eV. Hartke and Regensburger[23] have attempted to explain the shift in amorphous selenium by proposing the existance of an exciton 0.08 eV below the band gap of 2.53 eV. They did not discuss the photo-conduction edge in hexagonal selenium. It would not be expected to find strong exciton absorption in the non-crystalline modification if it did not also exist in the crystalline form. Grunwald and others[36] have observed electron and hole trapping levels in macroscopic electrical conductivity and charge transport measurements. Using a band model, these levels have been thought to exist just above and just below the conduction and valence band.

Previous band models for amorphous selenium have been concerned only with energy levels without any consideration for the point symmetry of a particular atom.

A band model with such symmetry is proposed here. It must be emphasized that the meaning of a band model in this amorphous material has a different meaning from that usually associated with a perfect crystal. The space group symmetry used is identical to that of hexagonal selenium. The symmetry directions, however, are referred to a few atoms in some small, localized region of space. There is absolutely no correlation between a direction in $\vec{k}$-space and a direction in the amorphous sample. The existence of short range hexagonal structure in the amorphous form is used as the basis for proposing such a band model to describe the energy levels for a small number of atoms in the amorphous network which makes up the macroscopic sample.

For this reason it is necessary to distinguish macroscopic from microscopic properties. Optical absorption is a microscopic property of a solid since it is primarily atomic in origin. The atomic levels of an atom are influenced by the presence of the other atoms in the solid, but only one electron is excited by a single photon. Measurements of charge transport and other electrical properties are macroscopic since the motion of the electron or hole in the entire solid is examined. A band model is proposed below which shows the short range band scheme. The same model is used to

describe the macroscopic properties only with the understanding that these are controlled primarily by one direction, namely the chain direction.

As an aid to the discussion which follows, a diagram of the first Brillouin zone for hexagonal selenium is shown in Fig. 13. The notation for labeling the points of high symmetry is the same convention as used by Herman[43]. We assume that the band shape along the Γ-A direction is the same as that calculated by Olechna and Knox[42] as shown in the reduced zone of Fig. 14. Because the atoms are bound so tightly along the chains and so weakly bound in the plane containing Γ, M, and K, the bands in this plane will tend to be quite narrow. Hulin's[45] results for hexagonal tellurium indicate that the extrema in the bands occur probably near the points marked H and L. From the considerations of the binding, we would expect that the bands in this direction would also be relatively narrow[44].

Let us postulate that the trapping levels observed in measurements of charge transport are actually levels in other directions in $\vec{k}$-space than the chain directions. These levels will then be localized in small regions of the sample. Taking recent data from Grunwald's[36] measurements for samples made under similar conditions, we postulate that a minimum in the conduction band exists 0.34 eV below the minimum at A, and that a maximum in the

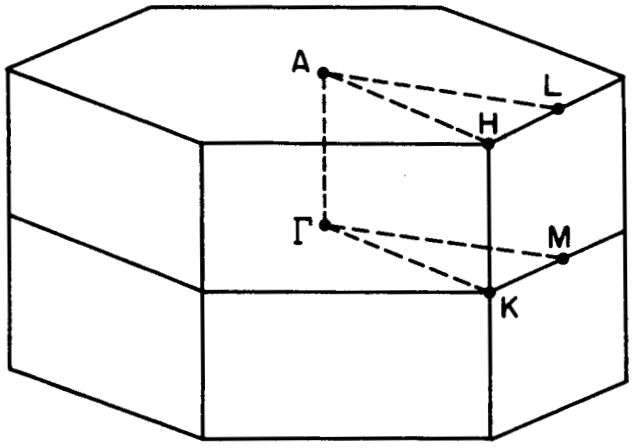

Fig. 13. First Brillouin zone of hexagonal Se (after Herman, Ref. 43)

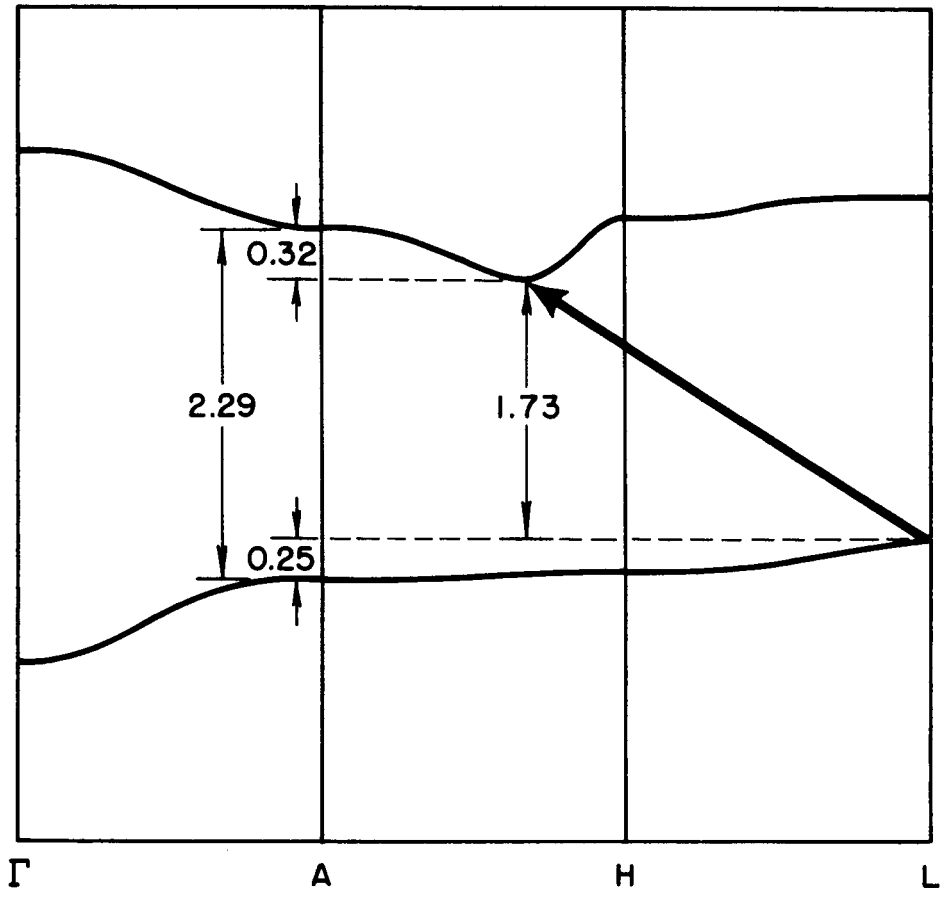

Fig. 14. Hypothetical band model for amorphous Se (all energies in ev)

valence band will be found 0.25 eV above the level at A. These two energies correspond to the trapping levels for electrons and holes respectively. The locations of the extrema were chosen so as to agree in principle with Hulin's[45] results for tellurium. The rest of the bands were drawn fairly flat with a firm hand simply to complete the picture, since there is no experimental evidence for any levels other than those mentioned. These results combined with the value of the indirect band gap at room temperature of 1.72 eV gives the direct gap at A as 2.29 eV. This result is 0.34 eV greater than the results of Olechna and Knox's calculation[42], and 0.24 eV smaller than the value used by Hartke and Regensburger[23]. It should be remembered that this band model has been based on the samples evaporated onto substrates held at 53°C. It would not be surprising to find different results for other substrate temperatures. The former difference is undoubtedly due to the differences in the second neighbor distances for the two forms of selenium being considered, and the second difference may be due to the somewhat arbitrary choice of the energies of the extrema relative to the direct gap at A. It is apparently fortunate that the band extrema in Hulin's calculation[45] were found in regions of the first Brillouin zone where $\vec{k}$ is large. The very small domains ($\sim$10Å) of hexagonal

order would limit the validity of this model severly were it not for the large $\vec{k}$ values or short wavelengths associated with these energy levels. Even the small size of the domains will not be a limitation because of coherence problems.

This band model seems to incorporate many experimental observations for the first time. First, and most important, it shows that absorption by indirect transitions will control the low energy region of the fundamental edge. Second, it shows that these transitions will not produce electrons or holes which will be free to conduct because of the small coherence region. Third, it shows that as the amorphous selenium is transformed into the hexagonal form, the absorption will produce carriers that will be able to move throughout the crystal. Finally, this model shows how the structure and amount of order affect the trapping levels to a certain degree. There remain many questions that cannot be fully explained until improvements have been made on the rather crude beginning for this model, however. Some suggested investigations which will add to this model are discussed in the following chapter.

CHAPTER VI

CONCLUSIONS AND SUGGESTIONS FOR FUTURE WORK

The absorption-edge spectrum of amorphous selenium has been measured at several temperatures below room temperature. Previous results which led to speculation about Urbach's rule were not observed. Structure seen in the spectrum was interpreted by the band theory in the manner used for other semiconductors. The results indicated that an indirect band gap and formation of indirect excitons were the cause of the onset of strong absorption. Results of other experiments and recent band calculations were used to draw a hypothetical energy band structure for the material.

As in many experiments, a few findings raise an even larger number of questions and ideas for other experiments. The rather novel suggestion of a band structure with definite symmetry needs considerable work toward further confirmation. Good single crystals of hexagonal selenium have recently become available. This makes the more simple crystalline phase the obvious starting place for further studies of selenium. The indirect band gap has been observed in hexagonal selenium, but no mention of excitons has been made to this author's knowledge. That they appear in the amorphous modification and not in the crystalline form would be surprising

indeed. Perhaps neutron diffraction would provide some information about the phonon spectrum as an aid to locating the band extrema.

Grunwald's results have indicated a shift in the trapping levels for films evaporated at different substrate temperatures. The effect of substrate temperature on the indirect band gap should give some further idea about the connection between trapping levels and the band extrema. The relation between the momentum source term and substrate temperature would also be interesting to observe since this term in the expression for the absorption coefficient is related to the amount of disorder in the sample.

The difficulty in fitting the coefficient of the indirect exciton term to any theoretical expression warrants further investigation. Such a study would undoubtedly require experimental apparatus with less possibility for error. It may be necessary to measure the reflectivity near normal incidence for all temperatures to be able to determine the low level absorption more accurately than in this experiment. The reflectivity spectrum at higher energies would also be helpful in locating positions of bands which do not contribute directly to the onset of absorption.

Cyclotron resonance, magneto-absorption and other

measurements in magnetic fields should add greatly to our knowledge of the band structure of selenium. The necessity of orienting the symmetry axes of the material with respect to the magnetic field in many experiments may require the use of good single crystals.

Amorphous selenium exhibits many properties common to all glasses. In particular, above the glass transition temperature[46] ($\sim 305^{\circ}K$), many parameters such as the volume coefficient of expansion change irregularly. This transition is evidently caused by a change in the structure or order which might be studied by the optical properties when they are better understood.

APPENDIX

CURVE FITTING TECHNIQUES

The laborious task of fitting theoretical absorption curves to experimental data has been eased somewhat by use of the IBM 7074 computer. The technique is essentially that used when fitting the curves by hand. The form of the theoretical equations allows them to be cast into nearly linear equations by taking the appropriate root. A least squares technique yields the slope and intercept of the linear equation which best fit the data.

Let the expression to be fit be of the form

$$\alpha_{th} = \sum_{\ell=1}^{m} C_\ell (E-E_\ell)^{n}$$

The problem involved in using a least squares fit is that each E_ℓ is usually different, but each term is zero until $E \geq E_\ell$. Therefore for $E < E_2$ the expression

$$\alpha_{th}^{1/n_1} = C_1 (E-E_1)$$

will be linear in α^{1/n_1} and E . Since the origin of the next higher term has yet to be determined, only an unknown number of data points should be used. The program used a predetermined number of points n which would be used as a first attempt at fitting the line using a standard least squares technique. The fit was then extended once as long as the next point did not

exceed some fraction F of the mean deviation for the first n points.

The values of $\alpha_{th1} = C_1 (E-E_1)^{1/2}$ were calculated for the entire range of the data, and a new set of experimental points

$$\alpha_{exp}^{1/2} = \left[\alpha_{data} - \alpha_{th1} \right]^{1/2} = \left[\alpha_{data} - \sum_{\ell} C_\ell (E-E_\ell)^{1/2} \right]^{1/2}$$

were calculated. For α_{exp} greater than some α_{min} the least squares fit for the next term was determined in the same way until all of the curve had been fit.

The accuracy of the fit was controlled by the adjustment of the parameters α_{min} and F. The program could automatically adjust either one or both of these unitl an acceptable mean deviation had been achieved, or the operator could adjust them from run to run. For ease in interpretation, the Calcomp II plotter was used to compare the data and the fitted curve graphically, and numerical comparison was provided by the calculated mean deviation.

REFERENCES

1. G. G. Macfarlane, T. P. McLean, J. E. Quarrington, and V. Roberts, Phys. Rev. 108, 1377 (1957).
2. G. G. Macfarlane, T. P. McLean, J. E. Quarrington, and V. Roberts, Proc. Phys. Soc. Lond. 71, 683 (1958).
3. G. G. Macfarlane, T. P. McLean, J. E. Quarrington, and V. Roberts, J. Phys. Chem. Solids 8, 388 (1959).
4. G. G. Macfarlane, T. P. McLean, J. E. Quarrington, and V. Roberts, Phys. Rev. 111, 1245 (1958).
5. G. Dresselhaus, A. F. Kip, and C. Kittel Phys. Rev. 98, 368 (1955).
6. For a review of experimental methods used to determine band structure see B. Lax, Rev. Mod. Phys. 30, 122 (1958).
7. H. Richter and F. Herre, Z. Naturforsch. 13A, 874 (1958).
8. M. E. Straumanis, Z. Krist, 102, 432 (1940).
9. J. Dresner, J. Phys. Chem. Solids, 25, 505 (1964).
10. For a review and references to earlier work see T. S. Moss Optical Properties of Semi-Conductors (Butterworths Scientific Publications, London, 1959), Chapter 11.
11. W. F. Koehler, F. K. Odencrantz, and W. C. White, J. Opt. Soc. Am. 49, 109 (1959).

12. R. S. Caldwell and H. Y. Fan, Phys. Rev. 114, 664 (1959).

13. H. Gobrecht and A. Tausend, Z. Physik 161, 205 (1961).

14. S. Kandare, Compt. Rend. 244, 571 (1957).

15. N. N. Pribytkova, Optika i Spektroskopiya 2, 633 (1957).

16. A review of the absorption from 0.13Å to 150 is given by A. Vasko, J. Opt. Soc. Am. 55, 894 (1965).

17. W. E. Spear, Proc. Phys. Soc. Lond. B70, 669 (1957).

18. W. E. Spear, Proc. Phys. Soc. Lond. B76, 826 (1960).

19. H. P. D. Lanyon and W. E. Spear, Proc. Phys. Soc. Lond. 77, 1157 (1961).

20. J. Dresner, J. Chem. Phys. 35, 1628 (1961).

21. J. L. Hartke, Phys. Rev. 125, 1177 (1962).

22. H. P. D. Lanyon, Phys. Rev. 130, 134 (1963).

23. J. L. Hartke and P. J. Regensburger Phys. Rev. (to be published).

24. T. P. McLean in A. F. Gibson, F. A. Kroger, and R. E. Burgess, Progress in Semiconductors, Vol. 5 (John Wiley and Sons Inc., New York, 1960) p. 53.

25. R. S. Knox, Theory of Excitons, in Seitz and Turnbull Solid State Physics, supplement 5 (Academic Press, New York, 1963).

26. S. Tolansky Multiple-Beam Interferometry of Surfaces and Films (University Press, Oxford 1948). Chapter V.

27. Trade name of polychlorotrifluoroethylene plastic polymer made and supplied by the Fluorocarbon Company, Anaheim, California.

28. Supplied by Hastings and Co., Inc., Philadelphia, Pennsylvania.

29. M. A. Gilleo J. Chem. Phys. 19, 1291 (1951).

30. J. Stuke, Z. Phys., Lpz. 134, 194 (1953).

31. E. W. Saker, Proc. Phys. Soc. Lond. B65, 785 (1952).

32. C. Hilsum, Proc. Phys. Soc. Lond. B69, 506 (1956).

33. J. J. Dowd Proc. Phys. Soc. Lond. B64, 783 (1951).

34. See reference 24 p. 155.

35. F. Urbach, Phys. Rev., 92, 1324 (1953).

36. H. P. Grunwald, Thesis, University of Rochester (1965).

37. W. J. Choyke and L. Patrick Phys. Rev. 108, 25 (1957).

38. F. Eckart and W. Henrion, Phys. Stat. Sol. 2, 841 (1962).

39. G. G. Macfarlane and V. Roberts, Phys. Rev. 97, 1714 (1955).

40. G. G. Macfarlane and V. Roberts, Phys. Rev. 98, 1865 (1955).

41. I. Srb and A. Vasko, Czech, J. Phys. B13, 827 (1963).

42. D. J. Olechna and R. S. Knox, Phys. Rev. (to be published).

43. F. Herman, Rev. Mod. Phys. 30, 102 (1958).

44. R. S. Knox, private communication.

45. M. Hulin, Ann. Phys. 8, 647 (1963).

46. J. H. Gibbs, in J. D. Mackenzie Modern Aspects of the Vitreous State, Vol. I, p. 152 (Butterworths, London, 1960).

ERRATA

Structure in the Optical Absorption Edge

of Amorphous Selenium

by

Dean B. McKenney

Page	Line	Correction
iii	3-t	inspriation should read inspiration
iv	2-b	justified should read made plausible
	11-b	nearly should read linearly
3	10-t	existence should read existence
11	6-b	$E_{ex}(0) = \frac{m^* e^4}{2\hbar^2 \varepsilon^2}$ should read $E_{ex}(0) = \frac{\mu^* e^4}{2\hbar^2 \varepsilon^2}$
	6-b	.... of the exciton in a medium of dielectric constant .
12	4-t	higher order should read other
	2-b	ref. 23,24 should read 24,25
17	12-t	colled should read cooled
24	4-b	The discussion in Chapter II would not lead one
31		Slopes of the curves from top to bottom are: 9×10^{-4} eV/°K, 10.9×10^{-4} eV/°K and 9×10^{-4} eV/°K.
41	14-b	Table I should read Table 1
	1-b	independant should read independent
44	8-t	inconsistancies should read inconsistencies
	2-b	correspondance should read correspondence

48	6-t	selenium, the minimum band gap .....
	8-t	calculation should read analysis
51	1-b	0.34 should read 0.32
62	ref. 25	Add: See also R. J. Elliott, Phys. Rev. 108, 1384 (1957) for original calculation
63	ref. 34	See reference 24 should read See reference 25.